

Chapter 3 – The Yee’s Finite-Difference Time-Domain (FDTD) Scheme for Maxwell’s Equations

3.1 Introduction

In this chapter a brief introduction of the procedure for applying finite-difference time-domain (FDTD) method to time-domain Maxwell equations is shown. Specifically the Yee’s FDTD formulation will be illustrated. In this chapter the Yee FDTD scheme will be restricted to a model with linear, non-dispersive and non-magnetic dielectric. Various considerations such as numerical dispersion, stability of the model and terminating the model with absorbing boundary condition (ABC) will be discussed. Extension of the Yee FDTD scheme to a general printed circuit board (PCB) environment will be discussed in Chapter 4. A FDTD software to implement all the algorithms in Chapter 3 and 4 will be shown in Chapter 5 and a more general stability theorem will be presented in Chapter 6.

3.2 Maxwell’s Equations and Initial Value Problem

Consider the general Maxwell’s equations in time domain including magnetic current density \vec{M} and magnetic charge density ρ_m (Balanis 1989):

$$\nabla \times \vec{E} = -\vec{M} - \frac{\partial}{\partial t} \vec{B} \quad (3.2.1a)$$

$$\nabla \times \vec{H} = \vec{J} + \frac{\partial}{\partial t} \vec{D} \quad (3.2.1b)$$

$$\nabla \cdot \vec{D} = \rho_e \quad (3.2.1c)$$

$$\nabla \cdot \vec{B} = \rho_m \quad (3.2.1d)$$

\vec{M} and ρ_m are equivalent sources since no magnetic monopole has been discovered to the best of the author’s knowledge. The other parameters for (3.2.1a)-(3.2.1d) are listed as follows:

\vec{E} - Electric field intensity

\vec{H} - Magnetic field intensity

\vec{D} - Electric flux density

\vec{B} - Magnetic flux density

ρ_e - Electric charge density

\vec{J} - Electric current density

Usually we will just call \vec{E} the electric field and \vec{H} the magnetic field. In (3.2.1a)-(3.2.1d), if the media is linear, we could introduce additional constitutive relations:

$$\vec{D} = \epsilon * \vec{E} \quad (3.2.2a)$$

$$\vec{B} = \mu * \vec{H} \quad (3.2.2b)$$

where ‘*’ indicates convolution operation in time (Balanis 1989). We would usually call ϵ the permittivity and μ the permeability of the media; both parameters are function of frequency ω . For a dispersionless medium, $\epsilon(\omega) = \epsilon$ and $\mu(\omega) = \mu$, (3.2.2a)-(3.2.2b) reduce to the form:

$$\vec{D} = \epsilon \vec{E} \quad (3.2.3a)$$

$$\vec{B} = \mu \vec{H} \quad (3.2.3b)$$

From the Maxwell’s equations, continuity relations for electric and magnetic current density can be derived. For instance from (3.2.1a):

$$\nabla \cdot (\nabla \times \vec{E}) = -\nabla \cdot \vec{M} - \nabla \cdot \left(\frac{\partial}{\partial t} \vec{B} \right) = 0$$

$$\Rightarrow \frac{\partial}{\partial t} (\nabla \cdot \vec{B}) = -\nabla \cdot \vec{M} = \frac{\partial}{\partial t} \rho_m$$

$$\nabla \cdot \vec{M} = -\frac{\partial}{\partial t} \rho_m \quad (3.2.4a)$$

Note that the vector identity $\nabla \cdot \nabla \times \vec{A} = 0$ is used. Similarly from (3.2.1b):

$$\nabla \cdot (\nabla \times \vec{B}) = \nabla \cdot \vec{J} + \nabla \cdot \left(\frac{\partial}{\partial t} \vec{D} \right) = 0$$

$$\Rightarrow \frac{\partial}{\partial t} (\nabla \cdot \vec{D}) = -\nabla \cdot \vec{J} = \frac{\partial}{\partial t} \rho_e$$

$$\nabla \cdot \vec{J} = -\frac{\partial}{\partial t} \rho_e \quad (3.2.4b)$$

Notice that in (3.2.1a)-(3.2.1d), only the curl equations (3.2.1a) for \vec{E} and (3.2.1b) for \vec{H} determine how the fields will change over time. This provides a clue that perhaps only these two equations are all that is needed to formulate a FDTD scheme. To obtain

a unique solution for the E and H fields of a system described by (3.2.1a)-(3.2.1d), additional information in the form of initial conditions and boundary conditions (if the domain is bounded) is required. First assuming an unbounded domain, then (3.2.1a)-(3.2.1d) together with the initial conditions for all the field components and sources $(\vec{J}, \vec{M}, \rho_e, \rho_m)$ constitute the initial value problem (IVP) for Maxwell's equations.

For simplicity suppose the model is a three-dimensional (3D) PCB assembly with linear, isotropic, non-dispersive dielectrics, and there is no magnetic charge and magnetic current $(\rho_m = 0, \vec{M} = 0)$. Also assume that initially all field components and sources are 0. Thus the following equations describe the IVP for the model:

$$\nabla \times \vec{E} = -\frac{\partial}{\partial t} \vec{B} \quad (3.2.5a)$$

$$\nabla \times \vec{H} = \vec{J} + \frac{\partial}{\partial t} \vec{D} \quad (3.2.5b)$$

$$\nabla \cdot \vec{D} = \rho_e \quad (3.2.5c)$$

$$\nabla \cdot \vec{B} = 0 \quad (3.2.5d)$$

$$\vec{E}(x, y, z, t)|_{t=0} = \vec{H}(x, y, z, t)|_{t=0} = \vec{J}(x, y, z, t)|_{t=0} = 0 \text{ and } \rho_e(x, y, z, t)|_{t=0} = 0 \quad (3.2.5e)$$

for all $(x, y, z) \in \mathbb{R}^3$ and $t > 0$. From (3.2.4b):

$$\rho_e(x, y, z, t) = -\int_0^t \nabla \cdot \vec{J}(x, y, z, \tau) d\tau + C_1$$

where C_1 is a constant. Using $\rho_e(x, y, z, t)|_{t=0} = 0$ and $\vec{J}(x, y, z, t)|_{t=0} = 0$ we see that $C_1 = 0$. Thus:

$$\rho_e(x, y, z, t) = -\int_0^t \nabla \cdot \vec{J}(x, y, z, \tau) d\tau \quad (3.2.6)$$

From (3.2.5a):

$$\nabla \cdot (\nabla \times \vec{E}) = -\nabla \cdot \left(\frac{\partial}{\partial t} \vec{B} \right) = 0 \Rightarrow \frac{\partial}{\partial t} (\nabla \cdot \vec{B}) = 0$$

Using the initial condition (3.2.5e), $\nabla \cdot \vec{B}|_{t=0} = \mu \nabla \cdot \vec{H}|_{t=0} = 0$, this implies that:

$$\nabla \cdot \vec{B}|_{t>0} = \nabla \cdot \vec{B}|_{t=0} = 0$$

Therefore the divergence equation for \vec{B} is implicit in (3.2.5a). In other words (3.2.5d) can be obtained from (3.2.5a) provided initial conditions (3.2.5e) applies. Now consider (3.2.5b):

$$\nabla \cdot (\nabla \times \vec{H}) = \nabla \cdot \vec{J} + \nabla \cdot \left(\frac{\partial \vec{D}}{\partial t} \right) = 0 \Rightarrow -\nabla \cdot \vec{J} = \frac{\partial}{\partial t} (\nabla \cdot \vec{D})$$

$$\nabla \cdot \vec{D} = - \int_0^t \nabla \cdot \vec{J} d\tau + C_2$$

Using the initial condition (3.2.5e), $\nabla \cdot \vec{D}|_{t=0} = \epsilon \nabla \cdot \vec{E}|_{t=0} = 0$, this implies that $C_2 = 0$.

Hence from (3.2.6):

$$\nabla \cdot \vec{D} = - \int_0^t \nabla \cdot \vec{J} d\tau = \rho_e$$

Again this shows that divergence equation for \vec{D} is implicit in (3.2.5b) provided initial conditions (3.2.5e) applies. From this argument, we see that the divergence equations (3.2.5c) and (3.2.5d) are redundant, thus the IVP of (3.2.5a)-(3.2.5e) can be reduced to:

$$\nabla \times \vec{E} = - \frac{\partial \vec{B}}{\partial t} \quad (3.2.7a)$$

$$\nabla \times \vec{H} = \vec{J} + \frac{\partial \vec{D}}{\partial t} \quad (3.2.7b)$$

$$\vec{E}(x, y, z, t)|_{t=0} = \vec{H}(x, y, z, t)|_{t=0} = \vec{J}(x, y, z, t)|_{t=0} = 0, \rho_e(x, y, z, t)|_{t=0} = 0 \quad (3.2.7c)$$

In general this is also true when the dielectric is dispersive and nonlinear, as long as the initial conditions for magnetic and electric flux densities fulfill $\nabla \cdot \vec{D}|_{t=0} = \nabla \cdot \vec{B}|_{t=0} = 0$.

This can also be extended to the case when magnetic current density \vec{M} and magnetic charge density ρ_m are present.

3.3 Yee's FDTD Formulation

Equations (3.2.7a)-(3.2.7c) form the basis of Yee's FDTD scheme (Yee 1966). There are a number of finite-difference schemes for Maxwell's equations, but the Yee scheme persists as it is very robust and versatile (Taflove 1995). Allowing for conduction electric current density $\vec{J} = \sigma \vec{E}$, (3.2.7a)-(3.2.7b) can be written as:

$$\frac{\partial \vec{E}}{\partial t} = \frac{1}{\epsilon} \nabla \times \vec{H} - \frac{\sigma}{\epsilon} \vec{E}$$

$$\frac{\partial \vec{H}}{\partial t} = -\frac{1}{\mu} \nabla \times \vec{E}$$

Under Cartesian coordinate system, these can be further expanded as:

$$\frac{\partial H_x}{\partial t} = -\frac{1}{\mu} \left(\frac{\partial E_z}{\partial y} - \frac{\partial E_y}{\partial z} \right) \quad (3.3.1a)$$

$$\frac{\partial H_y}{\partial t} = -\frac{1}{\mu} \left(\frac{\partial E_x}{\partial z} - \frac{\partial E_z}{\partial x} \right) \quad (3.3.1b)$$

$$\frac{\partial H_z}{\partial t} = -\frac{1}{\mu} \left(\frac{\partial E_y}{\partial x} - \frac{\partial E_x}{\partial y} \right) \quad (3.3.1c)$$

$$\frac{\partial E_x}{\partial t} = \frac{1}{\varepsilon} \left(\frac{\partial H_z}{\partial y} - \frac{\partial H_y}{\partial z} - \sigma E_x \right) \quad (3.3.1d)$$

$$\frac{\partial E_y}{\partial t} = \frac{1}{\varepsilon} \left(\frac{\partial H_x}{\partial z} - \frac{\partial H_z}{\partial x} - \sigma E_y \right) \quad (3.3.1e)$$

$$\frac{\partial E_z}{\partial t} = \frac{1}{\varepsilon} \left(\frac{\partial H_y}{\partial x} - \frac{\partial H_x}{\partial y} - \sigma E_z \right) \quad (3.3.1f)$$

Let us introduce the notation:

$$E_{x(i,j,k)}^n = E_x(i\Delta x, j\Delta y, k\Delta z, n\Delta t) \quad (3.3.2)$$

and so on for E_y, E_z, H_x, H_y and H_z components. In Yee's scheme, the model is first divided into many small cubes. For simplicity the cubes are assumed to be same size. The edges of each cube will form the three-dimensional space grid. The Yee's scheme can be generalized to variable cube size and non-orthogonal grid (Taflove 1995). The position of the E and H field components in the space grid is shown in Figure 3.1.

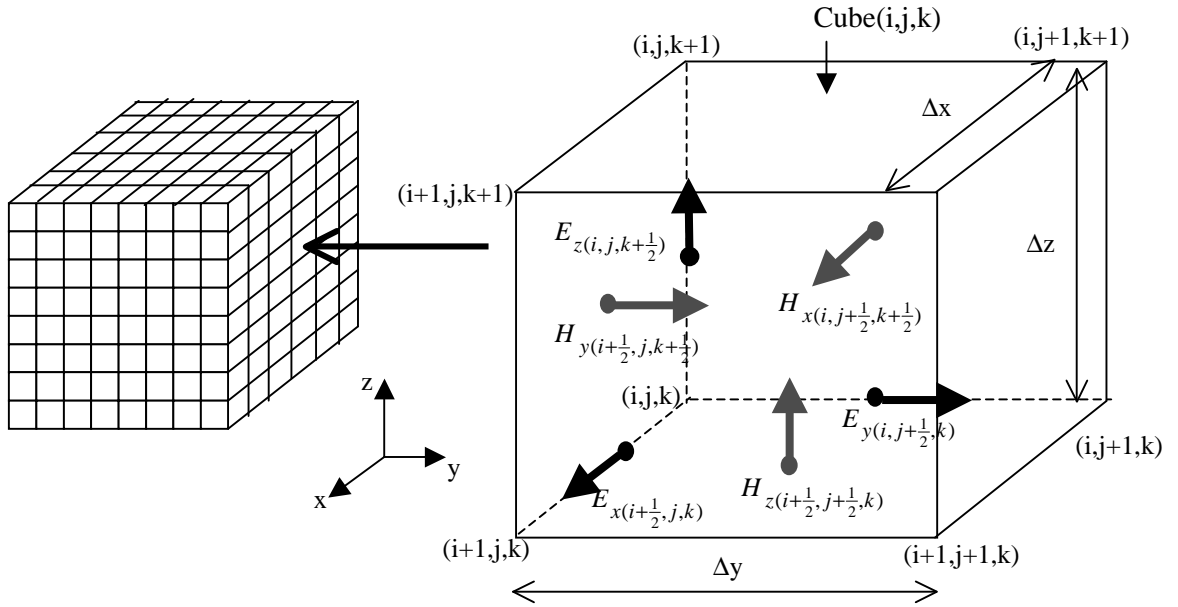


Figure 3.1 – Discretization of the model into cubes and the position of field components on the grid.

The cube in Figure 3.1 is usually called the Yee Cell. From Figure 3.1, it is observed that each E field component is surrounded by four H field components, similarly each H field component is surrounded by four E field components (If the field components on adjacent cubes are taken into account). For example, the component $H_{x(i,j+\frac{1}{2},k+\frac{1}{2})}$ is surrounded by $E_{z(i,j,k+\frac{1}{2})}$, $E_{z(i,j+1,k+\frac{1}{2})}$, $E_{y(i,j+\frac{1}{2},k)}$ and $E_{y(i,j+\frac{1}{2},k+1)}$. The inspiration for choosing this arrangement stems from the curl equations (3.2.7a)-(3.2.7b). As an example converting (3.2.7a) into integral form after using Stokes Theorem:

$$\oint_C \vec{E} \cdot d\vec{l} = -\frac{\partial}{\partial t} \iint_S \vec{B} \cdot d\vec{s}$$

This equation states that a changing magnetic flux will generate a circular electric field surrounding the ‘flux tube’. Similarly the integral form of (3.2.7b) also states that a changing electric flux and an electric current will generate a circular magnetic field

surrounding the ‘flux tube’. Using the center difference operator to replace the time and space derivatives at time-step n and space lattice point $(i\Delta x, (j + \frac{1}{2})\Delta y, (k + \frac{1}{2})\Delta z)$ on (3.3.1a):

$$\begin{aligned} \frac{1}{\Delta t} \left(H_{x(i, j+\frac{1}{2}, k+\frac{1}{2})}^{n+\frac{1}{2}} - H_{x(i, j+\frac{1}{2}, k+\frac{1}{2})}^{n-\frac{1}{2}} \right) &= \frac{-1}{\mu} \left(\frac{1}{\Delta y} \left(E_{z(i, j+\frac{1}{2}, k+\frac{1}{2})}^n - E_{z(i, j, k+\frac{1}{2})}^n \right) \right. \\ &\quad \left. - \frac{1}{\Delta z} \left(E_{y(i, j+\frac{1}{2}, k+1)}^n - E_{y(i, j+\frac{1}{2}, k)}^n \right) \right) \\ \Rightarrow H_{x(i, j+\frac{1}{2}, k+\frac{1}{2})}^{n+\frac{1}{2}} &= H_{x(i, j+\frac{1}{2}, k+\frac{1}{2})}^{n-\frac{1}{2}} - \frac{\Delta t}{\mu} \left(\frac{E_{z(i, j+\frac{1}{2}, k+\frac{1}{2})}^n - E_{z(i, j, k+\frac{1}{2})}^n}{\Delta y} - \frac{E_{y(i, j+\frac{1}{2}, k+1)}^n - E_{y(i, j+\frac{1}{2}, k)}^n}{\Delta z} \right) \end{aligned} \quad (3.3.3a)$$

Repeating this procedure for (3.3.1d) at time-step $n + \frac{1}{2}$ and space lattice point

$((i + \frac{1}{2})\Delta x, j\Delta y, k\Delta z)$:

$$\begin{aligned} \frac{1}{\Delta t} \left(E_{x(i+\frac{1}{2}, j, k)}^{n+1} - E_{x(i+\frac{1}{2}, j, k)}^n \right) &= \frac{1}{\varepsilon \Delta y} \left(H_{z(i+\frac{1}{2}, j+\frac{1}{2}, k)}^{n+\frac{1}{2}} - H_{z(i+\frac{1}{2}, j-\frac{1}{2}, k)}^{n+\frac{1}{2}} \right) \\ - \frac{1}{\varepsilon \Delta z} \left(H_{y(i+\frac{1}{2}, j, k+\frac{1}{2})}^{n+\frac{1}{2}} - H_{y(i+\frac{1}{2}, j, k-\frac{1}{2})}^{n+\frac{1}{2}} \right) &- \frac{1}{\varepsilon} \sigma E_{x(i+\frac{1}{2}, j, k)}^{n+\frac{1}{2}} \end{aligned}$$

Substituting $E_{x(i, j, k)}^{n+\frac{1}{2}}$ with the average between time-step n and $n+1$:

$$\begin{aligned} \frac{1}{\Delta t} \left(E_{x(i+\frac{1}{2}, j, k)}^{n+1} - E_{x(i+\frac{1}{2}, j, k)}^n \right) &= \frac{1}{\varepsilon \Delta y} \left(H_{z(i+\frac{1}{2}, j+\frac{1}{2}, k)}^{n+\frac{1}{2}} - H_{z(i+\frac{1}{2}, j-\frac{1}{2}, k)}^{n+\frac{1}{2}} \right) \\ - \frac{1}{\varepsilon \Delta z} \left(H_{y(i+\frac{1}{2}, j, k+\frac{1}{2})}^{n+\frac{1}{2}} - H_{y(i+\frac{1}{2}, j, k-\frac{1}{2})}^{n+\frac{1}{2}} \right) &- \frac{1}{\varepsilon} \sigma \cdot \frac{1}{2} \left(E_{x(i+\frac{1}{2}, j, k)}^{n+1} + E_{x(i+\frac{1}{2}, j, k)}^n \right) \end{aligned}$$

After some algebraic manipulation, we obtained:

$$\begin{aligned} E_{x(i+\frac{1}{2}, j, k)}^{n+1} &= \left(\frac{1 - \frac{\sigma \Delta t}{2\varepsilon}}{1 + \frac{\sigma \Delta t}{2\varepsilon}} \right) E_{x(i+\frac{1}{2}, j, k)}^{n+1} \\ &+ \frac{\frac{\Delta t}{\varepsilon}}{1 + \frac{\sigma \Delta t}{2\varepsilon}} \left(\frac{H_{z(i+\frac{1}{2}, j+\frac{1}{2}, k)}^{n+\frac{1}{2}} - H_{z(i+\frac{1}{2}, j-\frac{1}{2}, k)}^{n+\frac{1}{2}}}{\Delta y} - \frac{H_{y(i+\frac{1}{2}, j, k+\frac{1}{2})}^{n+\frac{1}{2}} - H_{y(i+\frac{1}{2}, j, k-\frac{1}{2})}^{n+\frac{1}{2}}}{\Delta z} \right) \end{aligned} \quad (3.3.3b)$$

By the same token, the update equations for the other field components can be derived:

$$H_{y(i+\frac{1}{2},j,k+\frac{1}{2})}^{n+\frac{1}{2}} = H_{y(i+\frac{1}{2},j,k+\frac{1}{2})}^{n-\frac{1}{2}} - \frac{\Delta t}{\mu} \left(\frac{E_{x(i+\frac{1}{2},j,k+1)}^n - E_{x(i+\frac{1}{2},j,k)}^n}{\Delta z} - \frac{E_{z(i+1,j,k+\frac{1}{2})}^n - E_{z(i,j,k+\frac{1}{2})}^n}{\Delta x} \right) \quad (3.3.3c)$$

$$H_{z(i+\frac{1}{2},j+\frac{1}{2},k)}^{n+\frac{1}{2}} = H_{z(i+\frac{1}{2},j+\frac{1}{2},k)}^{n-\frac{1}{2}} - \frac{\Delta t}{\mu} \left(\frac{E_{y(i+1,j+\frac{1}{2},k)}^n - E_{y(i,j+\frac{1}{2},k)}^n}{\Delta x} - \frac{E_{x(i+\frac{1}{2},j+1,k)}^n - E_{x(i+\frac{1}{2},j,k)}^n}{\Delta y} \right) \quad (3.3.3d)$$

$$E_{y(i,j+\frac{1}{2},k)}^{n+1} = \left(\frac{1-\frac{\sigma\Delta t}{2\varepsilon}}{1+\frac{\sigma\Delta t}{2\varepsilon}} \right) E_{y(i,j+\frac{1}{2},k)}^{n+1} + \frac{\frac{\Delta t}{\varepsilon}}{1+\frac{\sigma\Delta t}{2\varepsilon}} \left(\frac{H_{x(i,j+\frac{1}{2},k+\frac{1}{2})}^{n+\frac{1}{2}} - H_{x(i,j+\frac{1}{2},k-\frac{1}{2})}^{n+\frac{1}{2}}}{\Delta z} - \frac{H_{z(i+\frac{1}{2},j+\frac{1}{2},k)}^{n+\frac{1}{2}} - H_{z(i-\frac{1}{2},j+\frac{1}{2},k)}^{n+\frac{1}{2}}}{\Delta x} \right) \quad (3.3.3e)$$

$$E_{z(i,j,k+\frac{1}{2})}^{n+1} = \left(\frac{1-\frac{\sigma\Delta t}{2\varepsilon}}{1+\frac{\sigma\Delta t}{2\varepsilon}} \right) E_{z(i,j,k+\frac{1}{2})}^{n+1} + \frac{\frac{\Delta t}{\varepsilon}}{1+\frac{\sigma\Delta t}{2\varepsilon}} \left(\frac{H_{y(i+\frac{1}{2},j,k+\frac{1}{2})}^{n+\frac{1}{2}} - H_{y(i-\frac{1}{2},j,k+\frac{1}{2})}^{n+\frac{1}{2}}}{\Delta x} - \frac{H_{x(i,j+\frac{1}{2},k+\frac{1}{2})}^{n+\frac{1}{2}} - H_{x(i,j-\frac{1}{2},k+\frac{1}{2})}^{n+\frac{1}{2}}}{\Delta y} \right) \quad (3.3.3f)$$

Examination of (3.3.3a)-(3.3.3f) shows that all the field components fall on the locations accounted for by the space grid of Figure 3.1. Equations (3.3.3a)-(3.3.3f) are explicit in nature, thus computer implementation does not require solving for determinant or inverse of a large matrix. To facilitate the implementation in digital computer, the indexes of the field components are renamed as shown in Figure 3.2, so that all the indexes become integers. This allows the value of each field component to be stored in a three-dimensional array in the software, with the array indexes correspond to the spatial indexes of Figure 3.2. In the figure additional field components are drawn to improve the clarity of the convention.

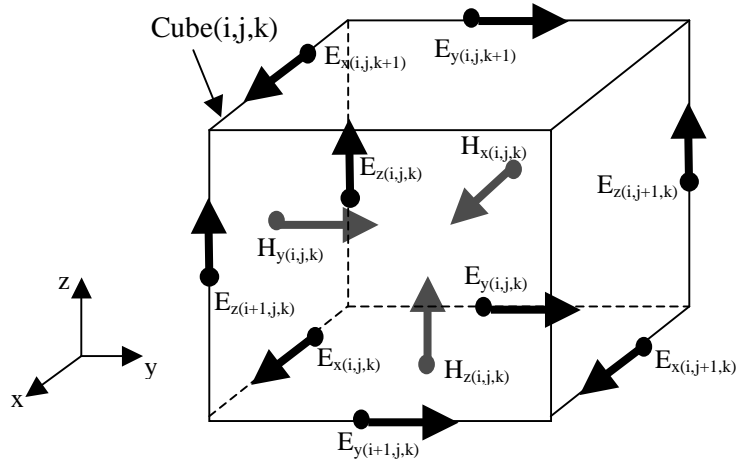


Figure 3.2 – Renaming the indexes of E and H field components corresponding to Cube (i,j,k).

Using the new spatial indexes for field components as in Figure 3.2, (3.3.3a)-(3.3.3f) become:

$$H_{x(i,j,k)}^{n+\frac{1}{2}} = H_{x(i,j,k)}^{n-\frac{1}{2}} - \frac{\Delta t}{\mu} \left(\frac{E_{z(i,j,k+1)}^n - E_{z(i,j,k)}^n}{\Delta y} - \frac{E_{y(i,j,k+1)}^n - E_{y(i,j,k)}^n}{\Delta z} \right) \quad (3.3.4a)$$

$$H_{y(i,j,k)}^{n+\frac{1}{2}} = H_{y(i,j,k)}^{n-\frac{1}{2}} - \frac{\Delta t}{\mu} \left(\frac{E_{x(i,j,k+1)}^n - E_{x(i,j,k)}^n}{\Delta z} - \frac{E_{z(i+1,j,k)}^n - E_{z(i,j,k)}^n}{\Delta x} \right) \quad (3.3.4b)$$

$$H_{z(i,j,k)}^{n+\frac{1}{2}} = H_{z(i,j,k)}^{n-\frac{1}{2}} - \frac{\Delta t}{\mu} \left(\frac{E_{y(i+1,j,k)}^n - E_{y(i,j,k)}^n}{\Delta x} - \frac{E_{x(i,j+1,k)}^n - E_{x(i,j,k)}^n}{\Delta y} \right) \quad (3.3.4c)$$

$$E_{x(i,j,k)}^{n+1} = \left(\frac{1 - \frac{\sigma \Delta t}{2\epsilon}}{1 + \frac{\sigma \Delta t}{2\epsilon}} \right) E_{x(i,j,k)}^n + \frac{\Delta t}{1 + \frac{\sigma \Delta t}{2\epsilon}} \left(\frac{H_{z(i,j,k)}^{n+\frac{1}{2}} - H_{z(i,j-1,k)}^{n+\frac{1}{2}}}{\Delta y} - \frac{H_{y(i,j,k)}^{n+\frac{1}{2}} - H_{y(i,j,k-1)}^{n+\frac{1}{2}}}{\Delta z} \right) \quad (3.3.4d)$$

$$E_{y(i,j,k)}^{n+1} = \left(\frac{1 - \frac{\sigma \Delta t}{2\epsilon}}{1 + \frac{\sigma \Delta t}{2\epsilon}} \right) E_{y(i,j,k)}^n + \frac{\Delta t}{1 + \frac{\sigma \Delta t}{2\epsilon}} \left(\frac{H_{x(i,j,k)}^{n+\frac{1}{2}} - H_{x(i,j,k-1)}^{n+\frac{1}{2}}}{\Delta z} - \frac{H_{z(i,j,k)}^{n+\frac{1}{2}} - H_{z(i-1,j,k)}^{n+\frac{1}{2}}}{\Delta x} \right) \quad (3.3.4e)$$

$$E_{z(i,j,k)}^{n+1} = \left(\frac{1 - \frac{\sigma \Delta t}{2\varepsilon}}{1 + \frac{\sigma \Delta t}{2\varepsilon}} \right) E_{z(i,j,k)}^n + \frac{\frac{\Delta t}{\varepsilon}}{1 + \frac{\sigma \Delta t}{2\varepsilon}} \left(\frac{H_{y(i,j,k)}^{n+\frac{1}{2}} - H_{y(i-1,j,k)}^{n+\frac{1}{2}}}{\Delta x} - \frac{H_{x(i,j,k)}^{n+\frac{1}{2}} - H_{x(i,j-1,k)}^{n+\frac{1}{2}}}{\Delta y} \right) \quad (3.3.4f)$$

Equations (3.3.4a)-(3.3.4f) form the basis of computer implementation of Yee's FDTD scheme for IVP of Maxwell's equations. Since (3.3.4a)-(3.3.4f) compute the new field components from the field components at previous time-steps, these equations are frequently called update equations. Notice that in the equations the temporal location of the E and H field components differs by half time-step ($\frac{1}{2} \Delta t$). In a typical simulation flow, one would determine the new H field components at $n + \frac{1}{2}$ from the previous field components using (3.3.4a)-(3.3.4c). Then the new E field components at $n + 1$ will be calculated using (3.3.4d)-(3.3.4f). The process is then repeated as many times as required until the last time-step is reached. Because of this, the scheme is sometimes called leapfrog scheme in some literatures. The details of implementation will be shown in Section 3.6. To show that the divergence equations (3.2.5c) and (3.2.5d) are implicit in (3.3.4a)-(3.3.4f), consider $\frac{1}{\Delta x} (E_{x(i,j,k)}^{n+1} - E_{x(i-1,j,k)}^{n+1})$. Assuming ε , μ and σ are homogeneous and using (3.3.4d), this can be written as:

$$\begin{aligned} \frac{1}{\Delta x} (E_{x(i,j,k)}^{n+1} - E_{x(i-1,j,k)}^{n+1}) &= \left(\frac{1 - \frac{\sigma \Delta t}{2\varepsilon}}{1 + \frac{\sigma \Delta t}{2\varepsilon}} \right) (E_{x(i,j,k)}^n - E_{x(i,j-1,k)}^n) \frac{1}{\Delta x} \\ &+ \frac{\frac{\Delta t}{\varepsilon}}{1 + \frac{\sigma \Delta t}{2\varepsilon}} \left(\frac{H_{z(i,j,k)}^{n+\frac{1}{2}} - H_{z(i,j-1,k)}^{n+\frac{1}{2}}}{\Delta y} - \frac{H_{y(i,j,k)}^{n+\frac{1}{2}} - H_{y(i,j,k-1)}^{n+\frac{1}{2}}}{\Delta z} \right) \frac{1}{\Delta x} \\ &- \frac{\frac{\Delta t}{\varepsilon}}{1 + \frac{\sigma \Delta t}{2\varepsilon}} \left(\frac{H_{z(i-1,j,k)}^{n+\frac{1}{2}} - H_{z(i-1,j-1,k)}^{n+\frac{1}{2}}}{\Delta y} - \frac{H_{y(i-1,j,k)}^{n+\frac{1}{2}} - H_{y(i-1,j,k-1)}^{n+\frac{1}{2}}}{\Delta z} \right) \frac{1}{\Delta x} \end{aligned} \quad (3.3.5a)$$

Similar terms can be written for E_x and E_y field components.

$$\begin{aligned}
\frac{1}{\Delta y} \left(E_{y(i,j,k)}^{n+1} - E_{y(i,j-1,k)}^{n+1} \right) &= \left(\frac{1 - \frac{\sigma \Delta t}{2\epsilon}}{1 + \frac{\sigma \Delta t}{2\epsilon}} \right) \left(E_{y(i,j,k)}^n - E_{y(i,j-1,k)}^n \right) \frac{1}{\Delta y} \\
&+ \frac{\frac{\Delta t}{\epsilon}}{1 + \frac{\sigma \Delta t}{2\epsilon}} \left(\frac{H_{x(i,j,k)}^{n+\frac{1}{2}} - H_{x(i,j,k-1)}^{n+\frac{1}{2}}}{\Delta z} - \frac{H_{z(i,j,k)}^{n+\frac{1}{2}} - H_{z(i-1,j,k)}^{n+\frac{1}{2}}}{\Delta x} \right) \frac{1}{\Delta y} \\
&- \frac{\frac{\Delta t}{\epsilon}}{1 + \frac{\sigma \Delta t}{2\epsilon}} \left(\frac{H_{x(i,j-1,k)}^{n+\frac{1}{2}} - H_{x(i,j-1,k-1)}^{n+\frac{1}{2}}}{\Delta z} - \frac{H_{z(i,j-1,k)}^{n+\frac{1}{2}} - H_{z(i-1,j-1,k)}^{n+\frac{1}{2}}}{\Delta x} \right) \frac{1}{\Delta y}
\end{aligned} \tag{3.3.5b}$$

$$\begin{aligned}
\frac{1}{\Delta z} \left(E_{z(i,j,k)}^{n+1} - E_{z(i,j,k-1)}^{n+1} \right) &= \left(\frac{1 - \frac{\sigma \Delta t}{2\epsilon}}{1 + \frac{\sigma \Delta t}{2\epsilon}} \right) \left(E_{z(i,j,k)}^n - E_{z(i,j,k-1)}^n \right) \frac{1}{\Delta z} \\
&+ \frac{\frac{\Delta t}{\epsilon}}{1 + \frac{\sigma \Delta t}{2\epsilon}} \left(\frac{H_{y(i,j,k)}^{n+\frac{1}{2}} - H_{y(i-1,j,k)}^{n+\frac{1}{2}}}{\Delta x} - \frac{H_{x(i,j,k)}^{n+\frac{1}{2}} - H_{x(i,j-1,k)}^{n+\frac{1}{2}}}{\Delta y} \right) \frac{1}{\Delta z} \\
&- \frac{\frac{\Delta t}{\epsilon}}{1 + \frac{\sigma \Delta t}{2\epsilon}} \left(\frac{H_{y(i,j,k-1)}^{n+\frac{1}{2}} - H_{y(i-1,j,k-1)}^{n+\frac{1}{2}}}{\Delta x} - \frac{H_{x(i,j,k-1)}^{n+\frac{1}{2}} - H_{x(i,j-1,k-1)}^{n+\frac{1}{2}}}{\Delta y} \right) \frac{1}{\Delta z}
\end{aligned} \tag{3.3.5c}$$

Summing up (3.3.5a)-(3.3.5c), the following equation is obtained.

$$\begin{aligned}
&\frac{E_{x(i,j,k)}^{n+1} - E_{x(i-1,j,k)}^{n+1}}{\Delta x} + \frac{E_{y(i,j,k)}^{n+1} - E_{y(i,j-1,k)}^{n+1}}{\Delta y} + \frac{E_{z(i,j,k)}^{n+1} - E_{z(i,j,k-1)}^{n+1}}{\Delta z} \\
&= \left(\frac{1 - \frac{\sigma \Delta t}{2\epsilon}}{1 + \frac{\sigma \Delta t}{2\epsilon}} \right) \left(\frac{E_{x(i,j,k)}^n - E_{x(i-1,j,k)}^n}{\Delta x} + \frac{E_{y(i,j,k)}^n - E_{y(i,j-1,k)}^n}{\Delta y} + \frac{E_{z(i,j,k)}^n - E_{z(i,j,k-1)}^n}{\Delta z} \right)
\end{aligned} \tag{3.3.6}$$

From (3.3.6), it is observed that if initially $E_{x(i,j,k)}^0 = E_{y(i,j,k)}^0 = E_{z(i,j,k)}^0 = 0$, for all i, j, k ,

then:

$$\frac{E_{x(i,j,k)}^{n+1} - E_{x(i-1,j,k)}^{n+1}}{\Delta x} + \frac{E_{y(i,j,k)}^{n+1} - E_{y(i,j-1,k)}^{n+1}}{\Delta y} + \frac{E_{z(i,j,k)}^{n+1} - E_{z(i,j,k-1)}^{n+1}}{\Delta z} = 0 \tag{3.3.7}$$

for all time-steps n . It is immediately recognized that (3.3.7) is actually the finite-difference equivalent of the divergence equation (3.2.5c) in free space. A similar procedure can also be applied to the H field components, obtaining:

$$\frac{H_{x(i+1,j,k)}^{n+\frac{1}{2}} - H_{x(i,j,k)}^{n+\frac{1}{2}}}{\Delta x} + \frac{H_{y(i,j+1,k)}^{n+\frac{1}{2}} - H_{y(i,j,k)}^{n+\frac{1}{2}}}{\Delta y} + \frac{H_{z(i,j,k+1)}^{n+\frac{1}{2}} - H_{z(i,j,k)}^{n+\frac{1}{2}}}{\Delta z} = 0 \tag{3.3.8}$$

Finally, it should be pointed out that the Yee's FDTD scheme is second order accurate due to the center-difference operator employed for approximating the differential operators. This means the truncation error for the center difference scheme is proportional to $(\Delta x^2, \Delta y^2, \Delta z^2, \Delta t^2)$, the determination of the truncation error is shown in Appendix 1. Before considering an actual computer implementation, the next section will address some special conditions encountered in PCB modeling.

3.4 Special Conditions

Perfect Electric Conductors

The boundary condition for a perfect electric conductor (PEC) requires the tangential E field to be zero at the boundary. Within the computational domain, all conductors must then be located on the electric field component. A PEC is modeled by setting the tangential E field components to zero where PEC is located. For example if there is a PEC on one of the surface of Cube (i,j,k) in Figure 3.3, the following E field components will be zero at all time-steps:

$$E_{x(i,j,k+1)}^n = E_{x(i,j+1,k+1)}^n = E_{y(i,j,k+1)}^n = E_{y(i+1,j,k+1)}^n = 0 \quad (3.4.1)$$

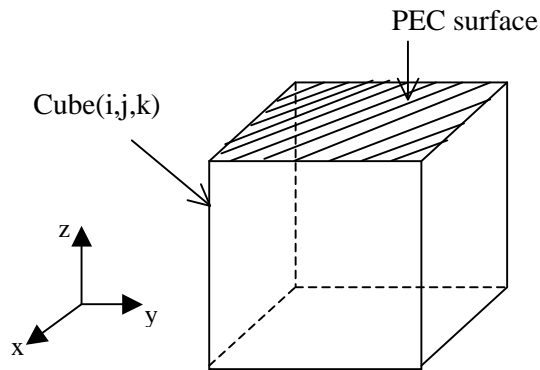


Figure 3.3 – An example with PEC on the top surface of Cube (i,j,k) .

Dielectric-Dielectric Interface

The boundary condition for dielectric-dielectric interface requires continuity of the tangential E and H fields across the boundary. Assuming the model is non-magnetic, $\mu(x, y, z) = \mu_0$. Because of this the interface plane must always locate on the E field component. The update equation for the corresponding E field will be slightly modified, taking into accounts the different permittivity and conductivity of adjacent cubes. The following shows the derivation of the update equation for E_x field component which is surrounded by four different dielectric cubes. Consider a closed loop C encircling $E_{x(i,j,k)}^n$ component. Loop C consists of four paths, S_1, S_2, S_3 and S_4 . Each path falls within a cube, let S_1 fall within Cube (i,j,k) , S_2 in Cube $(i,j-1,k)$, S_3 in Cube $(i,j-1,k-1)$ and S_4 in Cube $(i,j,k-1)$. This is shown in Figure 3.4 and Figure 3.5.

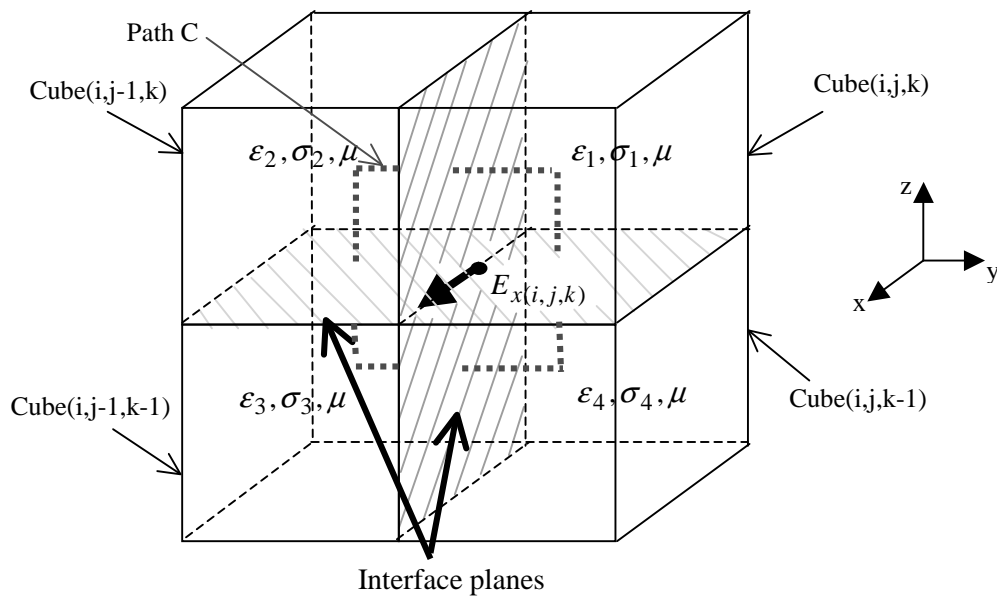


Figure 3.4 – Four adjacent cubes with different permittivity and conductivity.

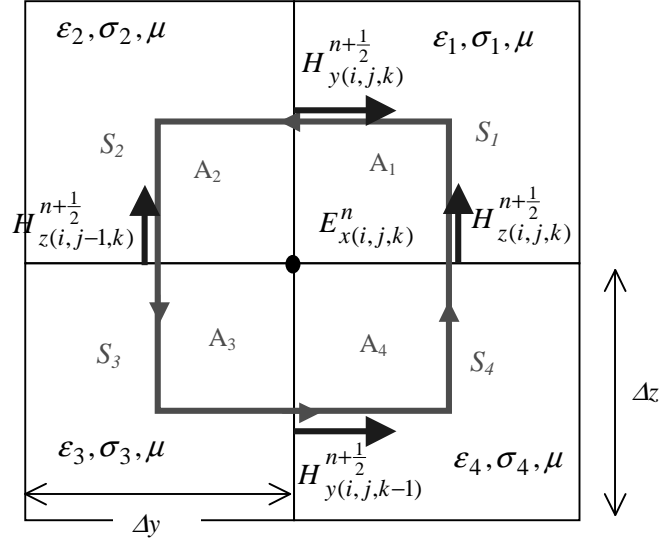


Figure 3.5 – A closed loop C crossing four cubes with different permittivity and conductivity.

Applying the integral form of $\frac{\partial \vec{E}}{\partial t} = \frac{1}{\epsilon} \nabla \times \vec{H} - \frac{\sigma}{\epsilon} \vec{E}$ along path C:

$$\oint_C \vec{H} \cdot d\vec{l} = \int_{S_1} \vec{H} \cdot d\vec{l} + \int_{S_2} \vec{H} \cdot d\vec{l} + \int_{S_3} \vec{H} \cdot d\vec{l} + \int_{S_4} \vec{H} \cdot d\vec{l} =$$

$$\iint_{A_1} \left(\epsilon_1 \frac{\partial \vec{E}}{\partial t} + \sigma_1 \vec{E} \right) \cdot d\vec{s} + \iint_{A_2} \left(\epsilon_2 \frac{\partial \vec{E}}{\partial t} + \sigma_2 \vec{E} \right) \cdot d\vec{s} + \iint_{A_3} \left(\epsilon_3 \frac{\partial \vec{E}}{\partial t} + \sigma_3 \vec{E} \right) \cdot d\vec{s} + \iint_{A_4} \left(\epsilon_4 \frac{\partial \vec{E}}{\partial t} + \sigma_4 \vec{E} \right) \cdot d\vec{s}$$

Using central-difference scheme for time and the procedure similar to derivation of (3.3.3b), this equation can be approximated as:

$$-\left(H_{y(i,j,k)}^{n+1/2} - H_{y(i,j,k-1)}^{n+1/2} \right) \Delta y + \left(H_{z(i,j,k)}^{n+1/2} - H_{z(i,j-1,k)}^{n+1/2} \right) \Delta z =$$

$$\left(\sigma_1 \cdot \frac{E_{x(i,j,k)}^{n+1} + E_{x(i,j,k)}^n}{2} + \epsilon_1 \frac{E_{x(i,j,k)}^{n+1} - E_{x(i,j,k)}^n}{\Delta t} \right) \frac{\Delta y \Delta z}{4}$$

$$+ \left(\sigma_2 \cdot \frac{E_{x(i,j,k)}^{n+1} + E_{x(i,j,k)}^n}{2} + \epsilon_2 \frac{E_{x(i,j,k)}^{n+1} - E_{x(i,j,k)}^n}{\Delta t} \right) \frac{\Delta y \Delta z}{4}$$

$$+ \left(\sigma_3 \cdot \frac{E_{x(i,j,k)}^{n+1} + E_{x(i,j,k)}^n}{2} + \epsilon_3 \frac{E_{x(i,j,k)}^{n+1} - E_{x(i,j,k)}^n}{\Delta t} \right) \frac{\Delta y \Delta z}{4}$$

$$+ \left(\sigma_4 \cdot \frac{E_{x(i,j,k)}^{n+1} + E_{x(i,j,k)}^n}{2} + \epsilon_4 \frac{E_{x(i,j,k)}^{n+1} - E_{x(i,j,k)}^n}{\Delta t} \right) \frac{\Delta y \Delta z}{4}$$

Upon rearranging the terms, the general update equation for E_x field component surrounded by four different dielectric cubes is obtained:

$$E_{x(i,j,k)}^{n+1} = \left(\frac{1 - \frac{\sigma'}{2\varepsilon'}}{1 + \frac{\sigma'}{2\varepsilon'}} \right) E_{x(i,j,k)}^n + \frac{\frac{\Delta t}{\varepsilon'}}{1 + \frac{\sigma'}{2\varepsilon'}} \left(\frac{H_{z(i,j,k)}^{n+\frac{1}{2}} - H_{z(i,j-1,k)}^{n+\frac{1}{2}}}{\Delta y} - \frac{H_{y(i,j,k)}^{n+\frac{1}{2}} - H_{y(i,j,k-1)}^{n+\frac{1}{2}}}{\Delta z} \right) \quad (3.4.2a)$$

where:

$$\varepsilon' = \frac{\varepsilon_1 + \varepsilon_2 + \varepsilon_3 + \varepsilon_4}{4} \quad \text{and} \quad \sigma' = \frac{\sigma_1 + \sigma_2 + \sigma_3 + \sigma_4}{4} \quad (3.4.2b)$$

Similar procedure is applied to E_y and E_z field components. In general we could modify (3.3.4d)-(3.3.4f) to account for dielectric discontinuity by taking the permittivity and conductivity as the average of four adjacent cubes surrounding the E field component. Equation (3.4.2a)-(3.4.2b) automatically guarantees the continuity of the tangential E field component. Since there is no change in the permeability across the interface, this also ensures the continuity of H field components. A discontinuity of permeability can be handled in a similar manner with the interface coincide with the H field component. However it must be noted that the current structure of the spatial grid does not allow discontinuity of both permittivity and permeability to occur simultaneously (Hockanson 1994).

Terminating the Simulation Domain

A basic consideration with implementation of FDTD approach on computer is the amount of data generated. Clearly, no computer can store an unlimited amount of data, therefore the domain must be limited in size. The computational domain must be large enough to enclose the structure of interest, and a suitable boundary condition on the outer perimeter of the domain must be used to simulate its extension to infinity. If the computational domain is extended sufficiently far beyond all sources and scatterers, all waves will be outgoing at the boundary. The boundary usually coincides with the tangential E fields. All E field components on the boundary are expressed as a function of the field components within the computational domain. A suitably formulated boundary condition will absorb majority of the incident wave energy, allowing only a small amount to reflect back into the computational domain. This type of boundary

condition is known as the Absorbing Boundary Condition (ABC). ABC allows the researcher to simulate electromagnetic fields interaction in an unbounded region on a computer with finite memory. A survey of ABC techniques is carried out extensively in Taflove (1995). The second type of boundary condition deliberately reflects all incident wave energy back into the computational domain, thus limiting the size of the computational domain. A typical boundary condition of this type is the PEC boundary condition, where on the boundary all the tangential E field components are perpetually fixed as zero.

The theories and formulations of some highly effective ABC can be found in Taflove (1995) and Kunz and Luebbers (1993). Here only the formulation concerning the ABC used in this thesis is discussed. The FDTD algorithm in this thesis uses a combination of the Mur's ABC and the PEC boundary. Mur's ABC is put forward by G. Mur in 1981 (Mur 1981), after the theoretical work by Engquist and Majda (1977). Mur's method relies on the fact that most of the electromagnetic waves will be outgoing at the boundary, as illustrated in Figure 3.6.

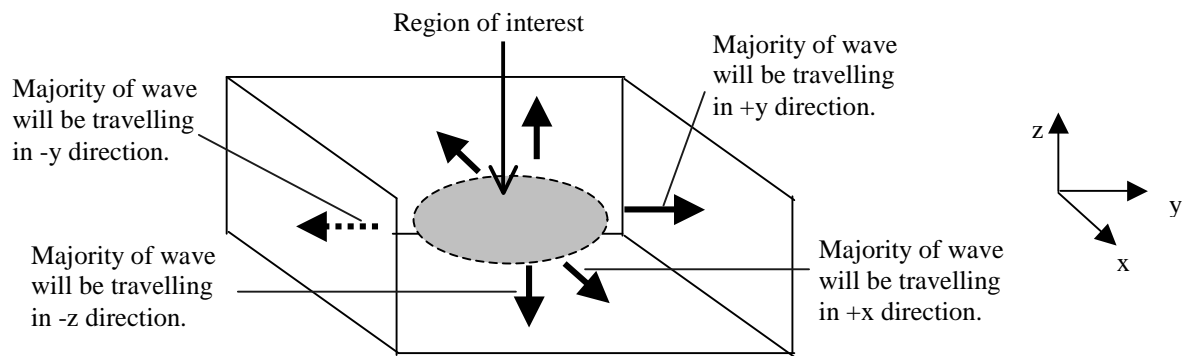


Figure 3.6 – Assumption of wave only propagates in one direction at a region sufficiently far from all sources and scatterers.

In Cartesian coordinate system, the wave equation for E field in an isotropic, homogeneous, source-free region is given by:

$$\left(\frac{\partial^2}{\partial x^2} + \frac{\partial^2}{\partial y^2} + \frac{\partial^2}{\partial z^2} - \frac{1}{c^2} \frac{\partial^2}{\partial t^2} \right) \vec{E} = 0 \quad (3.4.3a)$$

$$\frac{1}{c^2} = \mu\epsilon = s_x^2 + s_y^2 + s_z^2 \quad (3.4.3b)$$

In (3.4.3b), s_x , s_y and s_z are parameters that depend on the propagation direction of the E field. The linear partial differential operation of (3.4.3a) can be factorized into:

$$\left(\frac{\partial^2}{\partial x^2} + \frac{\partial^2}{\partial y^2} + \frac{\partial^2}{\partial z^2} - \frac{1}{c^2} \frac{\partial^2}{\partial t^2} \right) \vec{E} = \left[\left(\frac{\partial}{\partial x} + s_x \frac{\partial}{\partial t} \right) \left(\frac{\partial}{\partial x} - s_x \frac{\partial}{\partial t} \right) + \left(\frac{\partial}{\partial y} + s_y \frac{\partial}{\partial t} \right) \left(\frac{\partial}{\partial y} - s_y \frac{\partial}{\partial t} \right) + \left(\frac{\partial}{\partial z} + s_z \frac{\partial}{\partial t} \right) \left(\frac{\partial}{\partial z} - s_z \frac{\partial}{\partial t} \right) \right] \vec{E} = 0 \quad (3.4.4)$$

Essentially this means that the E field consists of superposition of components that travels along x , y and z axes. Each operator in the bracket corresponds to one-way wave propagation in either positive or negative direction along the three Cartesian axes. Consider the boundary at $y = 0$ and assuming that there is only E_x and E_z field components travelling toward $y = 0$. Concentrating on E_x field component initially, a one-way wave equation travelling towards $-y$ can be written for E_x :

$$\left(\frac{\partial}{\partial y} - s_y \frac{\partial}{\partial t} \right) E_x = 0 \quad (3.4.5)$$

Making the substitution $s_y = \sqrt{\frac{1}{c^2} - s_x^2 - s_z^2}$ in (3.4.5):

$$\left(\frac{\partial}{\partial y} - \frac{1}{c} \sqrt{1 - (cs_x)^2 - (cs_z)^2} \frac{\partial}{\partial t} \right) E_x = 0$$

The radical can be approximated with Taylor expansion:

$$\sqrt{1-x} = 1 - \frac{x}{2} + (\text{higher order terms})$$

A first order approximation would result in:

$$\left(\frac{\partial}{\partial y} - \frac{1}{c} \frac{\partial}{\partial t} \right) E_x = 0 \quad (3.4.6)$$

To conform to the position of field components in the Yee Cell in Figure 3.1, equation (3.4.6) is discretized at time-step $n + \frac{1}{2}$ and space lattice point $\left(\left(i + \frac{1}{2} \right) \Delta x, \left(j + \frac{1}{2} \right) \Delta y, k \Delta z \right)$:

$$\frac{E_{x(i+\frac{1}{2},j+1,k)}^{n+\frac{1}{2}} - E_{x(i+\frac{1}{2},j,k)}^{n+\frac{1}{2}}}{\Delta y} - \frac{1}{c} \frac{E_{x(i+\frac{1}{2},j+\frac{1}{2},k)}^{n+1} - E_{x(i+\frac{1}{2},j+\frac{1}{2},k)}^n}{\Delta t} = 0$$

Using averaging operation to estimate the E_x components that do not coincide with the spatial and temporal stepping for E field components:

$$\frac{E_{x(i+\frac{1}{2},j+1,k)}^{n+1} + E_{x(i+\frac{1}{2},j+1,k)}^n}{2} - \frac{E_{x(i+\frac{1}{2},j,k)}^{n+1} + E_{x(i+\frac{1}{2},j,k)}^n}{2} = \frac{\Delta y}{c\Delta t} \left(\frac{E_{x(i+\frac{1}{2},j+1,k)}^{n+1} + E_{x(i+\frac{1}{2},j,k)}^{n+1}}{2} - \frac{E_{x(i+\frac{1}{2},j+1,k)}^n - E_{x(i+\frac{1}{2},j,k)}^n}{2} \right) \quad (3.4.7)$$

Let the $y = 0$ boundary corresponds to $j = 1$, then (3.4.7) can be rearranged as:

$$E_{x(i+\frac{1}{2},1,k)}^{n+1} = E_{x(i+\frac{1}{2},2,k)}^n + \frac{c\Delta t - \Delta y}{c\Delta t + \Delta y} \left(E_{x(i+\frac{1}{2},2,k)}^{n+1} - E_{x(i+\frac{1}{2},1,k)}^n \right)$$

Upon renaming the spatial indexes of the E_x field component according to Figure 3.2, the interpolation relation for E_x at the boundary of $y = 0$ is obtained:

$$E_{x(i,1,k)}^{n+1} = E_{x(i,2,k)}^n + \frac{c\Delta t - \Delta y}{c\Delta t + \Delta y} \left(E_{x(i,2,k)}^{n+1} - E_{x(i,1,k)}^n \right) \quad (3.4.8)$$

For E_z field component at $y = 0$ boundary, we simply replace every occurrence of E_x with E_z . Similar procedures can also be applied at the other boundaries. The collection of update equations for all E field components at the remaining boundaries using first order Mur's approach is shown below. We suppose that there are n_x , n_y and n_z cubes along x , y and z axes respectively.

At $x = 0$:

$$E_{y(1,j,k)}^{n+1} = E_{y(2,j,k)}^n + \frac{c\Delta t - \Delta x}{c\Delta t + \Delta x} \left(E_{y(2,j,k)}^{n+1} - E_{y(1,j,k)}^n \right) \quad (3.4.9a)$$

$$E_{z(1,j,k)}^{n+1} = E_{z(2,j,k)}^n + \frac{c\Delta t - \Delta x}{c\Delta t + \Delta x} \left(E_{z(2,j,k)}^{n+1} - E_{z(1,j,k)}^n \right) \quad (3.4.9b)$$

At $x = n_x \Delta x$:

$$E_{y(n_x+1,j,k)}^{n+1} = E_{y(n_x,j,k)}^n + \frac{c\Delta t - \Delta x}{c\Delta t + \Delta x} \left(E_{y(n_x,j,k)}^{n+1} - E_{y(n_x+1,j,k)}^n \right) \quad (3.4.9c)$$

$$E_{z(n_x+1,j,k)}^{n+1} = E_{z(n_x,j,k)}^n + \frac{c\Delta t - \Delta x}{c\Delta t + \Delta x} \left(E_{z(n_x,j,k)}^{n+1} - E_{z(n_x+1,j,k)}^n \right) \quad (3.4.9d)$$

At $y = 0$:

$$E_{z(i,1,k)}^{n+1} = E_{z(i,2,k)}^n + \frac{c\Delta t - \Delta y}{c\Delta t + \Delta y} \left(E_{z(i,2,k)}^{n+1} - E_{z(i,1,k)}^n \right) \quad (3.4.9e)$$

At $y = n_y \Delta y$:

$$E_{x(i,n_y+1,k)}^{n+1} = E_{x(i,n_y,k)}^n + \frac{c\Delta t - \Delta y}{c\Delta t + \Delta y} \left(E_{x(i,n_y,k)}^{n+1} - E_{x(i,n_y+1,k)}^n \right) \quad (3.4.9f)$$

$$E_{z(i,n_y+1,k)}^{n+1} = E_{z(i,n_y,k)}^n + \frac{c\Delta t - \Delta y}{c\Delta t + \Delta y} \left(E_{z(i,n_y,k)}^{n+1} - E_{z(i,n_y+1,k)}^n \right) \quad (3.4.9g)$$

At $z=0$:

$$E_{x(i,j,1)}^{n+1} = E_{z(i,j,2)}^n + \frac{c\Delta t - \Delta z}{c\Delta t + \Delta z} \left(E_{z(i,j,2)}^{n+1} - E_{z(i,j,1)}^n \right) \quad (3.4.9h)$$

$$E_{y(i,j,1)}^{n+1} = E_{y(i,j,2)}^n + \frac{c\Delta t - \Delta z}{c\Delta t + \Delta z} \left(E_{y(i,j,2)}^{n+1} - E_{y(i,j,1)}^n \right) \quad (3.4.9i)$$

At $z = n_z \Delta z$:

$$E_{x(i,j,n_z+1)}^{n+1} = E_{x(i,j,n_z)}^n + \frac{c\Delta t - \Delta z}{c\Delta t + \Delta z} \left(E_{x(i,j,n_z+1)}^{n+1} - E_{x(i,j,n_z)}^n \right) \quad (3.4.9j)$$

$$E_{y(i,j,n_z+1)}^{n+1} = E_{y(i,j,n_z)}^n + \frac{c\Delta t - \Delta z}{c\Delta t + \Delta z} \left(E_{y(i,j,n_z+1)}^{n+1} - E_{y(i,j,n_z)}^n \right) \quad (3.4.9k)$$

Equations (3.4.9a)-(3.4.9k) only provide zero reflections when the incident numerical wave is normal to the boundary. At oblique angle of incident, there will be some reflection back into the computational domain. An improved ABC can be obtained by retaining higher order terms in the Taylor series expansion of $\sqrt{1 - (cs_x)^2 - (cs_z)^2}$. A second order approximation to (3.4.5) is:

$$\left[\frac{\partial}{\partial y} - \left(\frac{1}{c} - \frac{c}{2} (s_x^2 + s_z^2) \right) \frac{\partial}{\partial t} \right] E_x = 0 \quad (3.4.10)$$

However we do not know the value of $s_x^2 + s_z^2$, so further manipulation is necessary to express it in terms of known values and operators. Differentiating (3.4.10) with respect to time and dividing by c :

$$\left[\frac{1}{c} \frac{\partial^2}{\partial y \partial t} - \frac{1}{c^2} \frac{\partial^2}{\partial t^2} + \frac{1}{2} (s_x^2 + s_z^2) \frac{\partial^2}{\partial t^2} \right] E_x = 0 \quad (3.4.11)$$

From (3.4.3a):

$$\begin{aligned} & \left[\frac{\partial^2}{\partial x^2} + \frac{\partial^2}{\partial y^2} + \frac{\partial^2}{\partial z^2} - (s_x^2 + s_y^2 + s_z^2) \frac{\partial^2}{\partial t^2} \right] E_x = 0 \\ \Rightarrow & \left[\frac{\partial^2}{\partial x^2} + \frac{\partial^2}{\partial z^2} - (s_x^2 + s_z^2) \frac{\partial^2}{\partial t^2} \right] E_x = \left(\frac{\partial^2}{\partial y^2} - s_y^2 \right) E_x = 0 \end{aligned}$$

$$\left(s_x^2 + s_z^2\right) \frac{\partial^2}{\partial t^2} E_x = \left(\frac{\partial^2}{\partial x^2} + \frac{\partial^2}{\partial y^2}\right) E_x$$

Since a E_x wave propagating along y -axis is assumed. Substituting this result in (3.4.11), the second order boundary equation is obtained:

$$\left[\frac{1}{c} \frac{\partial}{\partial y \partial t} - \frac{1}{c^2} \frac{\partial^2}{\partial t^2} + \frac{1}{2} \frac{\partial^2}{\partial x^2} + \frac{1}{2} \frac{\partial^2}{\partial y^2}\right] E_x = 0 \quad (3.4.12)$$

Again substituting the differential operators with finite-difference operators and interpolating the necessary components, it can be shown that at boundary $y = 0$ (corresponds to index $j = 1$), the following update equation for $E_{x(i,1,k)}^n$ resulted (Mur 1981).

$$\begin{aligned} E_{x(i,1,k)}^{n+1} = & -E_{x(i,2,k)}^{n-1} + \frac{c\Delta t - \Delta y}{c\Delta t + \Delta y} \left(E_{x(i,2,k)}^{n+1} + E_{x(i,1,k)}^{n-1}\right) + \frac{2\Delta y}{c\Delta t + \Delta y} \left(E_{x(i,2,k)}^n + E_{x(i,1,k)}^n\right) \\ & + \frac{1}{2} \cdot \frac{\Delta y (c\Delta t)^2}{c\Delta t + \Delta y} \left(\frac{E_{x(i+1,2,k)}^n - 2E_{x(i,2,k)}^n + E_{x(i-1,2,k)}^n}{\Delta x^2} + \frac{E_{x(i+1,1,k)}^n - 2E_{x(i,1,k)}^n + E_{x(i-1,1,k)}^n}{\Delta x^2} \right) \\ & \left(\frac{E_{x(i,2,k+1)}^n - 2E_{x(i,2,k)}^n + E_{x(i,2,k-1)}^n}{\Delta z^2} + \frac{E_{x(i,1,k+1)}^n - 2E_{x(i,1,k)}^n + E_{x(i,1,k-1)}^n}{\Delta z^2} \right) \end{aligned} \quad (3.4.13)$$

Physically (3.4.13) computes a weighted average of the surrounding fields and assigns this value to the boundary component. Similar update equations can be derived for tangential E field components at all six planar absorbing boundaries (Mur 1981). For the Mur's second order ABC, the necessary components are not available at the edge where two absorbing boundaries meet. In this case the first order Mur's ABC update equation has to be used for these E field components. In this thesis the Mur's first order ABC is used for the following reasons:

1. Mur's first order ABC can be applied to boundary with dielectric discontinuities. For boundary with dielectric discontinuity it is discovered that the application of Mur's second order ABC will cause large spurious wave component to be generated in the computational domain, which defeat the purpose of having an ABC with better absorbing property. This is shown in Figure 3.7 for $y = 0$ boundary with a discontinuous dielectric along z -axis. The reason for this is electromagnetic wave travels at different velocity for dielectric with different permittivity. Mur's second order ABC assumes all associated E field components to have similar permittivity

and velocity c , as can be seen in (3.4.13), which is not true when the boundary E field component is sandwiched between two different dielectrics. This results in substantial error during the interpolation process, which then propagates back to the computational domain.

2. Computationally Mur's first order ABC is much easier to implement.
3. For many PCB modeling problems, the spurious reflection from Mur's first order ABC is still acceptable as long as sufficient buffer cubes are allocated. More will be discussed on this in later chapter.

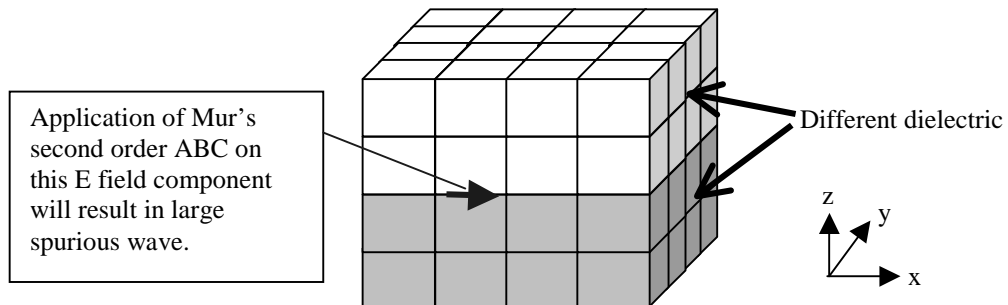


Figure 3.7 – Boundary E field component between two layers of different dielectrics.

As a final note on boundary condition, there are ABCs which are far more superior than Mur's approach. Most notably the Berenger's Perfectly Matched Layer (PML) (Berenger 1994) and its variants. However this will not be applied here due to the complexity of implementation and also the PML formulation will not work well with discontinuous dielectric on the boundary.

3.5 Other Considerations – Numerical Dispersion and Numerical Stability

Numerical Dispersion

The numerical algorithm for Maxwell's curl equations as defined by (3.3.4a)-(3.3.4f) causes dispersion of the simulated wave modes in the computational domain. For instance in vacuum, the phase velocity of the numerical wave modes in the FDTD grid can differ from vacuum speed of light. In fact the phase velocity of the numerical wave modes is a function of wavelength, the direction of propagation and the size of the cubes. This numerical dispersion can lead to nonphysical results such as broadening and ringing of single-pulse waveforms, imprecise canceling of multiple scattered wave and pseudorefraction. A detailed analysis of this numerical dispersion is presented in Chapter 5 of Taflove (1995) and thus will not be discussed here. It is shown in Taflove (1995) that to limit the amount of numerical dispersion, the edges of each cube must be at least ten times smaller than the shortest wavelength expected to propagate in the computational domain. Of course the numerical dispersion will be suppressed even further if smaller cube size is maintained. However using a cube size that is too small will increase the number of cubes needed to fill the computational domain and hence increase computational demand of the model. The rule-of-thumb of

$$\Delta x, \Delta y, \Delta z \leq \frac{\lambda_o}{10} \quad (3.5.1)$$

where λ_o is the expected highest significant harmonics in the model is adequate for most purposes.

Numerical Stability – The Courant-Friedrichs-Lewy Stability Criterion

The numerical algorithm for Maxwell's curl equations as defined by (3.3.4a)-(3.3.4f) requires that the time increment Δt have a specific bound relative to the spatial discretization Δx , Δy and Δz . For a linear, isotropic, non-dispersive and homogeneous dielectric with permittivity ϵ and permeability μ (the dielectric can have some losses in the form of non-zero conductivity σ), the time increment has to obey the following bound, known as Courant-Freidrichs-Lewy (CFL) Stability Criterion.

$$\Delta t < \frac{1}{c \sqrt{\frac{1}{\Delta x^2} + \frac{1}{\Delta y^2} + \frac{1}{\Delta z^2}}} \quad c = \frac{1}{\sqrt{\mu\epsilon}} \quad (3.5.2)$$

The model will not be stable if (3.5.2) is not obeyed. The definition for stability of Yee's FDTD scheme is similar to Definition 2.2 of Chapter 2. In an unstable model the computed result for E and H field components will increase without limit as the simulation progresses. This uncontrolled divergence of the field value is due to an artifact in the finite-difference method in general. The CFL Stability Criterion has many limitations:

1. It does not account for discontinuity in dielectric.
2. It assumes infinite domain. The effect of boundary condition on stability is not considered.
3. It only applies to linear dielectric and does not consider lumped linear and nonlinear models to be included in the model later.

Nevertheless the CFL Stability Criterion is still very useful. For model with a few different dielectric, as a rule-of-thumb c is taken as the largest value obtained from the various dielectrics. Derivation of (3.5.2) can be carried out using Von-Nuemann Analysis. The details are shown in Appendix 2.

3.6 Implementation of the Basic FDTD Algorithm

With all the details taken care of, Figure 3.8 shows the three-dimensional model and the convention for naming the cubes used in this thesis. Figure 3.9 illustrates the basic flow of implementing Yee's FDTD scheme on a computer. In Chapter 4, various considerations such as including lumped elements and adding voltage sources into the model will be discussed. However the basic flow still retains the same form as adding these components only changes the way the E field components are updated.

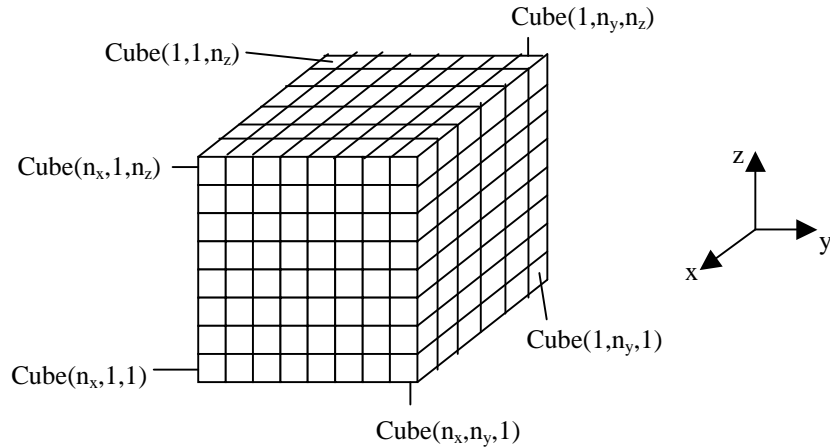


Figure 3.8 – The three-dimensional computational region for FDTD simulation.

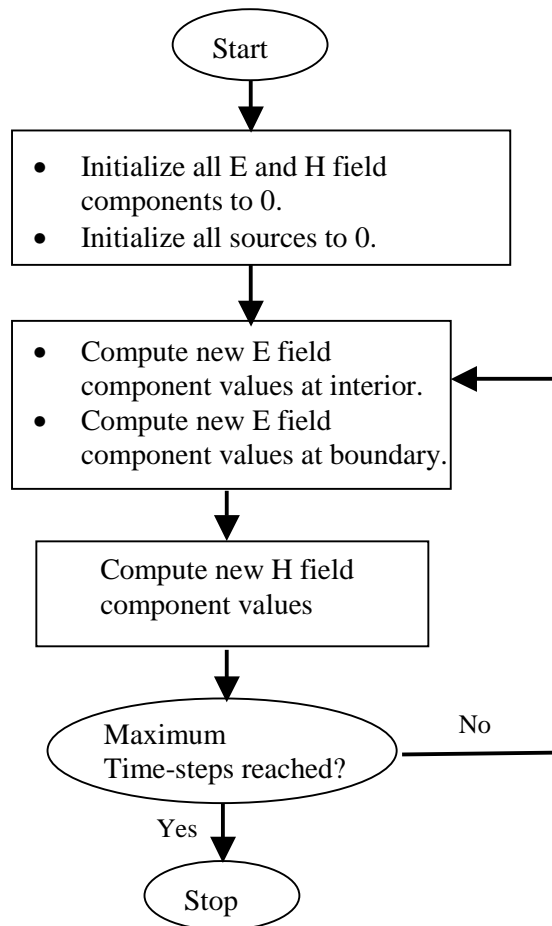


Figure 3.9 – Basic flow for implementation of Yee FDTD scheme.